Published in final edited form as:
Nat Med. 2008 January ; 14(1): 69–74. doi:10.1038/nm1682.

Recovery of supraspinal control of stepping via indirect propriospinal relay connections after spinal cord injury

Gregoire Courtine[1], **Bingbing Song**[2], **Roland R Roy**[1,3], **Hui Zhong**[1], **Julia E Herrmann**[2], **Yan Ao**[2], **Jingwei Qi**[2], **V Reggie Edgerton**[1,3], and **Michael V Sofroniew**[2,3]

[1]Department of Physiological Sciences, University of California, Los Angeles, California 90095-1763, USA.

[2]Department of Neurobiology, University of California, Los Angeles, California 90095-1763, USA.

[3]Brain Research Institute, University of California, Los Angeles, California 90095-1763, USA.

Abstract

Spinal cord injuries (SCIs) in humans[1,2] and experimental animals[3–6] are often associated with varying degrees of spontaneous functional recovery during the first months after injury. Such recovery is widely attributed to axons spared from injury that descend from the brain and bypass incomplete lesions, but its mechanisms are uncertain. To investigate the neural basis of spontaneous recovery, we used kinematic, physiological and anatomical analyses to evaluate mice with various combinations of spatially and temporally separated lateral hemisections with or without the excitotoxic ablation of intrinsic spinal cord neurons. We show that propriospinal relay connections that bypass one or more injury sites are able to mediate spontaneous functional recovery and supraspinal control of stepping, even when there has been essentially total and irreversible interruption of long descending supraspinal pathways in mice. Our findings show that pronounced functional recovery can occur after severe SCI without the maintenance or regeneration of direct projections from the brain past the lesion and can be mediated by the reorganization of descending and propriospinal connections[4,7–9]. Targeting interventions toward augmenting the remodeling of relay connections may provide new therapeutic strategies to bypass lesions and restore function after SCI and in other conditions such as stroke and multiple sclerosis.

Although spontaneous functional recovery after SCI is widely attributed to spared axons that descend from the brain past incomplete lesions, evidence has been presented periodically over the past 75 or more years suggesting that propriospinal connections may also make substantial contributions[10–14]. The degree to which propriospinal connections might mediate functional recovery after SCI has important implications for strategies to facilitate repair after SCI, but has thus far remained undetermined. In this study, we conducted a detailed kinematic, physiological and anatomical analysis of the basis for spontaneous recovery of hindlimb stepping after SCI in mice, using various combinations of SCI alone or SCI together with excitotoxic ablation of intrinsic spinal cord neurons.

Correspondence should be addressed to M.V.S. (sofroniew@mednet.ucla.edu). .

AUTHOR CONTRIBUTIONS G.C., R.R.R., V.R.E. and M.V.S. designed the experiments; G.C., B.S., R.R.R., H.Z., J.E.H., Y.A. and J.Q. performed the experiments; G.C., B.S., R.R.R., V.R.E. and M.V.S. analyzed the data and G.C., R.R.R., V.R.E. and M.V.S. wrote the paper.

Note: Supplementary information is available on the Nature Medicine website.

We first examined adult mice that received a single lateral (left) hemisection at thoracic segment 12 (T12; Fig. 1a) to test the effect of interrupting descending inputs to locomotor circuits at lumbar segments L1–L2 (ref. [15]) on one side (Figs. 1 and 2). Histological evaluations after these experiments consistently showed lesion-induced scarring through the entire ipsilateral dorsal-ventral extent of the spinal cord from the lateral margin to the midline (Supplementary Fig. 1 online), and completeness of the lesions was evaluated anatomically and functionally as described below. During the first week after this SCI, mice entirely lost the ability to step with (Fig. 1b,d,e and Supplementary Fig. 2 online) or recruit extensor (vastus lateralis) and flexor (tibialis anterior) muscles in the ipsilateral hindlimb (Fig. 1f,g), but retained the ability to step with the contralateral hindlimb (Fig. 1e and Supplementary Video 1 online). Bowel function was not detectably altered, and bladder function did not require assistance (that is, manual bladder expression) by the end of the first week after the unilateral hemisection (data not shown). Step-like movements began to reappear on the ipsilateral side by 10–14 d after injury, but gait analysis during treadmill locomotion at 14 d showed that mice were not able to take plantar steps with the ipsilateral hindlimb (Fig. 1d), had a significantly reduced stance duration (Supplementary Fig. 2a; within-subjects ANOVA, $P < 0.001$) and dragged the hindpaw during swing (Supplementary Fig. 2b and Supplementary Video 1). At 14 d after SCI, the tibialis anterior was strongly facilitated (Fig. 1g; ANOVA, $P < 0.001$) and coactivated (Fig. 1h) with the otherwise weakly active vastus lateralis (Fig. 1g; ANOVA, $P < 0.001$). From 2 to 7 weeks after injury, mice progressively recovered plantar stepping ability as evidenced by a lengthening in stance duration (Supplementary Fig. 2a) that correlated with an increase in vastus lateralis activity (Fig. 1f,g) and a decrease in paw-dragging duration (Supplementary Fig. 2b) associated with reduced (Fig. 1g) and coordinated (Fig. 1h) recruitment of flexor muscles (Supplementary Video 1).

To test the completeness of the lateral hemisection and to determine which of the descending anatomical pathways that regulate stepping either retained or regained connection with the ipsilateral locomotor circuits at L1–L2, we conducted quantitative retrograde tract-tracing (Fig. 2a–e). Mice injected with tracer immediately after SCI (acute group) and examined 1 week later showed pronounced and significant ($P < 0.001$) reductions in neuronal labeling of 75–100% in major brainstem motor centers (Fig. 2b,e) and in the spinal cord at T8–T10 (Fig. 2d,e), whereas neuronal labeling in the contralateral spinal cord caudal to the injury (L1–L2) was not significantly reduced (Fig. 2c,e) compared to uninjured mice. Mice injected with tracer 10 weeks after SCI (chronic group) showed no significant differences in neuronal labeling in the brainstem compared to mice injected with tracer immediately after SCI (Fig. 2e). However, propriospinal neuronal labeling in T8–T10 was significantly increased (ANOVA, $P < 0.01$) in mice injected at 10 weeks relative to mice injected immediately after SCI, with a return to about 40% of the amount seen in uninjured mice (Fig. 2d,e). To determine the time course of this increase, we examined additional mice injected with tracer at intermediate times and found that propriospinal neuronal labeling in T8–T10 increased gradually in mice injected at 2 and 4 weeks after unilateral hemisection SCI (Fig. 2e). Neuronal labeling in the contralateral spinal cord caudal to the injury at L1–L2 remained unaltered under the different experimental conditions (Fig. 2e).

To further test the completeness of the lateral hemisection at T12, we placed a second lateral hemisection 10 weeks after the first at the same level (T12) but on the contralateral side (Fig. 1c) in mice that had recovered from the first lesion. After this second lesion, mice showed complete paralysis of both hind limbs with no signs of recovery of locomotor function over 4 weeks ($n = 4$; Fig. 1e, Supplementary Fig. 2a,b and Supplementary Video 2), demonstrating that recovery after the first hemisection was due to supraspinal information passing the injury site on the contralateral side, rather than to the sparing of fibers ipsilateral to the hemisection or to autonomous activity of lumbosacral locomotor circuits.

Together, these findings showed that substantial recovery of hindlimb stepping with virtually normal coordinated recruitment between flexors and extensors had occurred spontaneously after an essentially complete lateral hemisection in which there was neither sparing nor regeneration of the original long-tract descending axons from the brain through the lesion to the ipsilateral locomotor circuits. This gradual restoration of kinematic and electromyographic (EMG) features of gait was accompanied by progressive anatomical changes in retrograde labeling compatible with either the gradual sprouting or recovery of spared intraspinal fibers or the gradual establishment of *de novo* relay propriospinal circuits connecting rostral T8–T10 neurons bilaterally to the caudal L1–L2 locomotor centers ipsilateral to the hemisection (Supplementary Fig. 3a–c,g online).

We next sought to identify essential components of the pathways mediating recovery. We examined mice that had received two spatially separated hemisections at T12 and T7 on opposite sides of the spinal cord to test the effect of transecting descending inputs from the brain to the locomotor circuits at L1–L2 on both sides while leaving an intervening gap of contiguous intrinsic spinal cord circuits (Figs. 2f and 3a). These two lesions were made either simultaneously or temporally separated by 10 weeks to allow time for recovery to plateau after the first hemisection, as described above. When the two lesions were placed simultaneously, mice showed complete bilateral hindlimb paralysis (Fig. 3b and Supplementary Fig. 4a online), the tibialis anterior was quiescent on both sides (Fig. 3c) and recovery over the 4 weeks postlesion was limited to small hindlimb movements on the T7 side (Fig. 3b, Supplementary Fig. 4a and Supplementary Video 3a online). We next examined the effects of first placing a hemisection at T12 and allowing the mice to recover ipsilateral stepping and then placing a second hemisection at T7 on the contralateral side 10 weeks after the T12 lesion (Figs. 2f and 3a). After this delayed second hemisection at T7, mice initially lost stepping ability completely on the T7 side and partially on the T12 side (Fig. 3b, Supplementary Fig. 4b and Supplementary Video 3b). After 3 d, the tibialis anterior muscle on the originally lesioned T12 side showed large, rhythmic bursts of EMG activity, whereas the tibialis anterior muscle on the newly lesioned T7 side was quiescent (Fig. 3c,d). Stepping ability returned gradually, and by 4 weeks after the delayed T7 hemisection, the mice had spontaneously recovered substantial and significant locomotor ability with voluntary treadmill and over-ground plantar stepping on both the T7 and the T12 sides (Fig. 3b, Supplementary Fig. 4b and Supplementary Video 3b). Bowel function was not detectably altered (data not shown). Manual bladder expression was required for all mice with delayed bilateral hemisections over the entire survival period, although about one-third of these mice showed some partial spontaneous bladder emptying (data not shown). We also examined the effects of a delayed complete spinal cord transection at T7 10 weeks after a hemisection at T12 (Fig. 3a). In these mice, there were no EMG bursts in the tibialis anterior (Fig. 3c,d), no hindlimb movements and no signs of recovery during the 4 weeks postlesion (Fig. 3b, Supplementary Fig. 4c and Supplementary Video 3c). Thus, the motor pool recruitment observed after the delayed T7 hemisection resulted from supraspinal drive being transferred past the lesion sites to the lumbosacral locomotor circuits, as opposed to autonomous, spinally generated muscle activity[16].

To determine whether descending anatomical pathways had remained intact or had regenerated after hemisections at T12 and T7, we injected retrograde tract-tracer bilaterally into the locomotor circuits at L1–L2 either immediately after simultaneous bilateral hemisections at T12 and T7 or 4 weeks after the delayed second hemisection at T7 (Fig. 2f). In comparison to uninjured mice, these mice all showed pronounced and significant ($P < 0.001$) reductions in neuronal labeling of 81–100% in brainstem motor centers, and there were no significant differences between mice receiving simultaneous or delayed double hemisections (Fig. 2g), indicating that the differences in locomotor behavior observed in these two groups of mice were not due to differences in the number of spared or regenerating supraspinal projections past the lesions. Notably, many propriospinal neurons at T8–T10 were retrogradely labeled in

a bilateral fashion by bilateral tracer injections at L1–L2 after either simultaneous or delayed lesions, and at 4 weeks after the delayed second hemisection at T7, the proportion of neurons showing this effect was about 40% of that in uninjured controls (Fig. 2g).

Together, these findings indicate that substantial recovery of bilateral hindlimb stepping function occurred after two temporally separated unilateral hemisections (at T12 and T7) that created an essentially complete bilateral transection of all direct projections from the brain to the locomotor circuits at L1–L2 but left an intervening bridge of intrinsic spinal cord circuitry (Supplementary Fig. 3c–e). The observation that recovery occurred when the lesions were placed at different times, but not after simultaneous lesions, suggested that recovery might be due to time-dependent changes such as reorganization of interactions between descending supraspinal connections and intrinsic spinal cord circuits able to relay information past the lesions.

To test further the role of thoracic propriospinal neurons above the lesion in mediating the functional recovery observed after a T12 hemisection (left), or after two temporally separated unilateral hemisections at T12 (left) and T7 (right), we ablated these neurons by infusing the axon-sparing excitotoxin *N*-methyl-D-aspartic acid (NMDA)[17] into the gray matter at T8 and T10 on the side of the T12 lesion (left) and at T9 on the side of the T7 lesion (right). These NMDA infusions ablated the majority of ipsilateral and contralateral neurons at the level of each injection (Fig. 4a). There was no detectable effect on the major myelinated long descending fiber tracts in the lateral portions of the lateral column, but, as expected, some degeneration and demyelination was observed among medial propriospinal fiber tracts after ablation of local propriospinal neurons (Fig. 4b). In otherwise uninjured mice, these NMDA infusions had only minor effects on hindlimb kinematics during stepping (Fig. 4c, Supplementary Fig. 5a and Supplementary Video 4a online), in agreement with findings by others[18].

In mice with a unilateral hemisection at T12 that had recovered stepping function after 10 weeks, infusions of NMDA completely abolished the spontaneously recovered stepping on the ipsilateral side and caused pronounced hyperextension and limb dragging with loss of trunk control, but these infusions did not significantly alter stepping on the side contralateral to the T12 hemisection (Fig. 4c, Supplementary Fig. 5b and Supplementary Video 4b). In mice with two temporally separated unilateral hemisections at T12 (left) and T7 (right) that had recovered bilateral stepping function 4 weeks after the second hemisection at T7, infusions of NMDA completely abolished the spontaneously recovered stepping on both sides and caused pronounced hyperextension and dragging of both hindlimbs (Fig. 4c, Supplementary Fig. 5c and Supplementary Video 4c). These findings showed that local thoracic propriospinal neurons were essential for the spontaneous recovery of bilateral stepping observed after a single hemisection or after two temporally and spatially separated hemisections, and any potentially spared long descending supraspinal fibers projecting past the lesion sites were not, on their own, sufficient to mediate supraspinal control of stepping (Supplementary Fig. 3f,h,i).

After complete spinal cord transection in both animals and humans, the intrinsic spinal cord circuitry is, with locomotor training, pharmacological administration or both, able to execute both standing and body weight–supported treadmill stepping in the complete absence of descending connections from the brain[19,20]. Recent studies have found substantial anatomical and physiological reorganization of descending and propriospinal circuits after partial descending-tract lesions[4,7–9]. *In vitro* organ preparations have revealed polysynaptic propriospinal circuits that are present at birth in mice and contribute to bulbospinal activation of locomotor networks in the lumbosacral spinal cord[21]. Our findings are compatible with, and substantially extend, these observations by showing that after severe SCI, full weight-bearing locomotion can be initiated voluntarily and sustained in the essential absence of inputs that

pass directly from the brain to the lumbosacral locomotor circuits and can be mediated by *de novo* relay propriospinal circuits that transmit neural information past the lesion sites. Thus, after SCI, the time-dependent reorganization and plasticity of long descending and propriospinal connections are sufficient to reestablish supraspinal control of lumbosacral circuits indirectly via relay connections that mediate substantial functional recovery.

The findings of this study have important implications for developing strategies to improve function after SCI (ref. [22]). Manipulations to promote axon regeneration and increase the sprouting and plasticity of residual connections are steadily improving[23–26] but little is known about which neural systems would be most effective to target with such interventions[27]. Our findings show that the precise restoration of point-to-point connections made by long-tract descending axons from the brain to the lumbosacral locomotor circuits is not required to achieve meaningful functional recovery. Instead, the reorganization of interactions between descending inputs and intrinsic spinal cord circuits that relay information past lesion sites is sufficient to achieve supraspinal control of lumbosacral circuits and recovery of function after severe SCI. Targeting interventions to augment the remodeling of relay connections should provide new, and potentially more easily achievable, therapeutic strategies to bypass lesions and restore function after SCI and in other debilitating conditions such as stroke and multiple sclerosis.

METHODS

Mice

Wild-type C57BL/6 female mice were derived from an in-house breeding colony. We housed the mice in a 12-h light-dark cycle in a specific pathogen–free facility with controlled temperature and humidity, and we allowed them free access to food and water. We conducted experiments according to protocols approved by the Chancellor's Animal Research Committee of the Office for Protection of Research Subjects at the University of California, Los Angeles.

Surgical procedures

We performed all surgical procedures on mice that were under full general anesthesia with isoflurane in oxygen-enriched air. We conducted basic surgical procedures and postoperative care for SCI subjects as described previously[28]. All descriptions of segmental levels refer to spinal cord levels. To selectively kill spinal cord neurons, we stereotaxically injected the excitotoxic glutamate agonist NMDA (Sigma) into the spinal cord gray matter at T8 and T10 on the side of the T12 lesion (left), and at T9 on the side of the T7 lesion (right), at a volume of 0.3 μl of 1 mM NMDA per site[17,28]. We conducted retrograde tract-tracing by injecting Dextran–Alexa 568 (3000 kDa; 2% w/v in sterile water) unilaterally or bilaterally into L1–L2 with glass micropipettes (100-μm tip) at 1 μl per site over 10 min with a Harvard microinfusion pump. We perfused the mice 1 week later and counted retrogradely labeled neurons as described[17,28].

Treadmill locomotion

We assessed hindlimb stepping function during continuous quadrupedal treadmill locomotion. We tested mice 0, 7, 14, 21, 28 and 48 d after SCI unless otherwise specified. The treadmill belt speed was set at 10.3 cm/s for all testing of T12-hemisected mice. We tested mice that had undergone double hemisection or NMDA infusion at 7.8 cm/s because they could not step at faster treadmill speeds.

Kinematics

Three-dimensional video recordings (100 Hz) were made with four cameras (Basler Vision Technologies) oriented at 45° and 135° with respect to the direction of the locomotion (that is,

the mouse's sagittal plane) on both sides. We attached reflective markers bilaterally to the shaved skin overlying specific bony landmarks (Fig. 1b). We used SIMI motion-capture software (SIMI Reality Motion Systems) to obtain three-dimensional coordinates of the markers. We modeled the body as an interconnected chain of rigid segments (Fig. 1b), and we generated the joint angles accordingly. Of note, the limb axis was the segment connecting the iliac crest to the metatarsal joint (toe). We extracted 10–15 consistent step cycles from a continuous sequence of stepping for each animal. We computed the amplitudes of joint and limb-axis motion as well as classic gait parameters[29].

Electromyograph recordings

Bipolar intramuscular EMG wires (AS631-2, Coonerwires) were implanted chronically into the vastus lateralis or tibialis anterior muscles bilaterally as described previously[29]. We routed the wires subcutaneously through the back to a small headplug (Fig. 1b; Omnetics) to which a light cable was attached during the recordings (Supplementary Fig. 2). We recorded (2,000 Hz), amplified and filtered (10–1,000 Hz band-pass) the EMG signals and computed the duration and mean amplitude of identified EMG bursts[29]. We generated probability density distributions of EMG amplitudes normalized to pre-lesion values of the antagonist tibialis anterior (flexor) and vastus lateralis (extensor) muscles during a sequence of 10 s of continuous treadmill stepping as described elsewhere[30].

Histological and morphometric procedures

After the final experiment, we processed the mice for histological evaluation as described[28]. We either stained the tissue sections with cresyl violet or evaluated them for the presence of retrograde tracer. We performed cell counts of retrogradely labeled neurons on tissue sections (coded so that the identity of the experimental group was hidden) with image analysis software (StereoInvestigator or NeuroLucida, MicroBrightField) operating a computer-driven microscope regulated in the *x*, *y* and *z* axes (Zeiss). We counted all retrogradely labeled neurons per section in a series of at least four evenly spaced sections through the entire region of each area analyzed and expressed the values as total number counted per region per mouse.

Statistics

We performed all statistical evaluations with one- or two-way ANOVA or repeated-measures ANOVA. We assessed *post hoc* pairwise differences by the Newman-Keuls test (Prism, GraphPad).

Supplementary Material

Refer to Web version on PubMed Central for supplementary material.

Acknowledgments

This work was supported by grants from the National Institutes of Health (NS16333), the Christopher and Dana Reeve Foundation, the Adelson Medical Foundation and the Roman Reed Spinal Cord Injury Research Fund of California.

References

1. Fawcett JW, et al. Guidelines for the conduct of clinical trials for spinal cord injury as developed by the ICCP panel: spontaneous recovery after spinal cord injury and statistical power needed for therapeutic clinical trials. Spinal Cord 2007;45:190–205. [PubMed: 17179973]
2. Dobkin B, et al. The evolution of walking-related outcomes over the first 12 weeks of rehabilitation for incomplete traumatic spinal cord injury: the multicenter randomized spinal cord injury locomotor trial. Neurorehabil. Neural Repair 2007;21:25–35. [PubMed: 17172551]

3. Weidner N, Ner A, Salimi N, Tuszynski M. Spontaneous corticospinal axonal plasticity and functional recovery after adult central nervous system injury. Proc. Natl. Acad. Sci. USA 2001;98:3513–3518. [PubMed: 11248109]
4. Bareyre FM, et al. The injured spinal cord spontaneously forms a new intraspinal circuit in adult rats. Nat. Neurosci 2004;7:269–277. [PubMed: 14966523]
5. Courtine G, et al. Performance of locomotion and foot grasping following a unilateral thoracic corticospinal tract lesion in monkeys (*Macaca mulatta*). Brain 2005;128:2338–2358. [PubMed: 16049043]
6. Ballermann M, Fouad K. Spontaneous locomotor recovery in spinal cord injured rats is accompanied by anatomical plasticity of reticulospinal fibers. Eur. J. Neurosci 2006;23:1988–1996. [PubMed: 16630047]
7. Raineteau O, Schwab ME. Plasticity of motor systems after incomplete spinal cord injury. Nat. Rev. Neurosci 2001;2:263–273. [PubMed: 11283749]
8. Kerschensteiner M, et al. Remodeling of axonal connections contributes to recovery in an animal model of multiple sclerosis. J. Exp. Med 2004;200:1027–1038. [PubMed: 15492125]
9. Jankowska E, Edgley SA. How can corticospinal tract neurons contribute to ipsilateral movements? A question with implications for recovery of motor functions. Neuroscientist 2006;12:67–79. [PubMed: 16394194]
10. Jane JA, Evans JP, Fisher LE. An investigation concerning the restitution of motor function following injury to the spinal cord. J. Neurosurg 1964;21:167–171. [PubMed: 14127616]
11. Basbaum AI. Conduction of the effects of noxious stimulation by short-fiber multisynaptic systems of the spinal cord in the rat. Exp. Neurol 1973;40:699–716. [PubMed: 4723852]
12. Stelzner DJ, Cullen JM. Do propriospinal projections contribute to hindlimb recovery when all long tracts are cut in neonatal or weanling rats? Exp. Neurol 1991;114:193–205. [PubMed: 1748194]
13. Duffy MT, Simpson SBJ, Liebich DR, Davis BM. Origin of spinal cord axons in the lizard regenerated tail: supernormal projections from local spinal neurons. J. Comp. Neurol 1990;293:208–222. [PubMed: 19189712]
14. Nantwi KD, El-Bohy AA, Schrimsher GW, Reier PJ, Goshgarian HG. Spontaneous recovery in a paralyzed hemidiaphragm following upper cervical spinal cord injury in adult rats. Neurorehabil. Neural Repair 1999;13:225–234.
15. Kiehn O. Locomotor circuits in the mammalian spinal cord. Annu. Rev. Neurosci 2006;29:279–306. [PubMed: 16776587]
16. Leblond H, L' Esperance M, Orsal D, Rossignol S. Treadmill locomotion in the intact and spinal mouse. J. Neurosci 2003;23:11411–11419. [PubMed: 14673005]
17. Sofroniew MV, Galletly NP, Isacson O, Svendsen CN. Survival of adult basal forebrain cholinergic neurons after loss of target neurons. Science 1990;247:338–342. [PubMed: 1688664]
18. Magnuson DS, et al. Comparing deficits following excitotoxic and contusion injuries in the thoracic and lumbar spinal cord of the adult rat. Exp. Neurol 1999;156:191–204. [PubMed: 10192790]
19. Fong AJ, et al. Spinal cord–transected mice learn to step in response to quipazine treatment and robotic training. J. Neurosci 2005;25:11738–11747. [PubMed: 16354932]
20. Edgerton VR, et al. Retraining the injured spinal cord. J. Physiol. (Lond.) 2001;533:15–22. [PubMed: 11351008]
21. Zaporozhets E, Cowley KC, Schmidt BJ. Propriospinal neurons contribute to bulbospinal transmission of the locomotor command signal in the neonatal rat spinal cord. J. Physiol. (Lond.) 2006;572:443–458. [PubMed: 16469789]
22. Courtine G, et al. Can experiments in nonhuman primates expedite the translation of treatments for spinal cord injury in humans? Nat. Med 2007;13:561–566. [PubMed: 17479102]
23. Schwab ME. Repairing the injured spinal cord. Science 2002;295:1029–1031. [PubMed: 11834824]
24. Filbin MT. Myelin-associated inhibitors of axonal regeneration in the adult mammalian CNS. Nat. Rev. Neurosci 2003;4:703–713. [PubMed: 12951563]
25. Silver J, Miller JH. Regeneration beyond the glial scar. Nat. Rev. Neurosci 2004;5:146–156. [PubMed: 14735117]

26. Irwin N, Li YM, O' Toole JE, Benowitz LI. Mst3b, a purine-sensitive Ste20-like protein kinase, regulates axon outgrowth. Proc. Natl. Acad. Sci. USA 2006;103:18320–18325. [PubMed: 17114295]

27. Thuret S, Moon LD, Gage FH. Therapeutic interventions after spinal cord injury. Nat. Rev. Neurosci 2006;7:628–643. [PubMed: 16858391]

28. Faulkner JR, et al. Reactive astrocytes protect tissue and preserve function after spinal cord injury. J. Neurosci 2004;24:2143–2155. [PubMed: 14999065]

29. Courtine G, et al. Kinematic and EMG determinants in quadrupedal locomotion of a non-human primate (*Rhesus*). J. Neurophysiol 2005;93:3127–3145. [PubMed: 15647397]

30. Recktenwald MR, et al. Effects of spaceflight on rhesus quadrupedal locomotion after return to 1G. J. Neurophysiol 1999;81:2451–2463. [PubMed: 10322080]

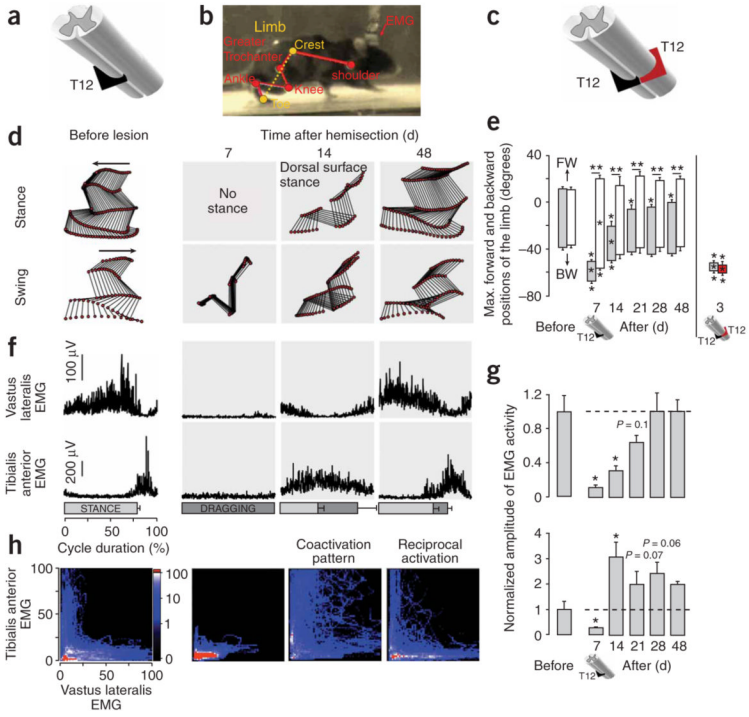

Figure 1.

Recovery of supraspinal control of stepping after a lateral hemisection at T12. (**a**) Schematic of left hemisection at T12 (black). (**b**) Reflective markers overlying bony landmarks were video recorded (100 Hz). The limb axis from iliac crest to toe (dashed line) was used to characterize forward and backward hindlimb oscillation. (**c**) Schematic of left hemisection at T12 (black) combined with a delayed right hemisection at the same level after 10 weeks (red). (**d**) Representative stick diagrams of ipsilateral hindlimb movements during stance and swing before and 7–48 d after left T12 hemisection. (**e**) Bar graphs representing the average maximum (Max) backward (BW) and forward (FW) angular positions of the limb axis depicted in **b** (*n* = 8). (**f**) Averaged EMG activity (*n* = 15 steps) for the vastus lateralis (extensor) and tibialis anterior (flexor) muscles ipsilateral to left T12 hemisection over the duration of the step cycle. Horizontal bars represent stance (light shading) or paw dragging (dark shading) durations. (**g**) Bar graphs representing the average EMG burst amplitude (*n* = 4 mice; 10 bursts per mouse) for vastus lateralis (top) and tibialis anterior (bottom) muscles ipsilateral to the hemisection at T12. (**h**) Probability density distributions (*n* = 4 mice, 10 steps per animal) of normalized EMG amplitudes in the vastus lateralis and anterior muscles during treadmill stepping. The L-shaped pattern observed during stepping before lesion indicates reciprocal activation between the antagonist anterior and vastus lateralis motor pools. The D-shape during stepping at 14 d after a T12 hemisection indicates co-activation between anterior and vastus lateralis. Values are means ± s.e.m. *$P < 0.01$ and ** $P < 0.001$ indicate a statistically significant differences between before and after lesion values and between ipsilateral and contralateral hindlimbs, respectively.

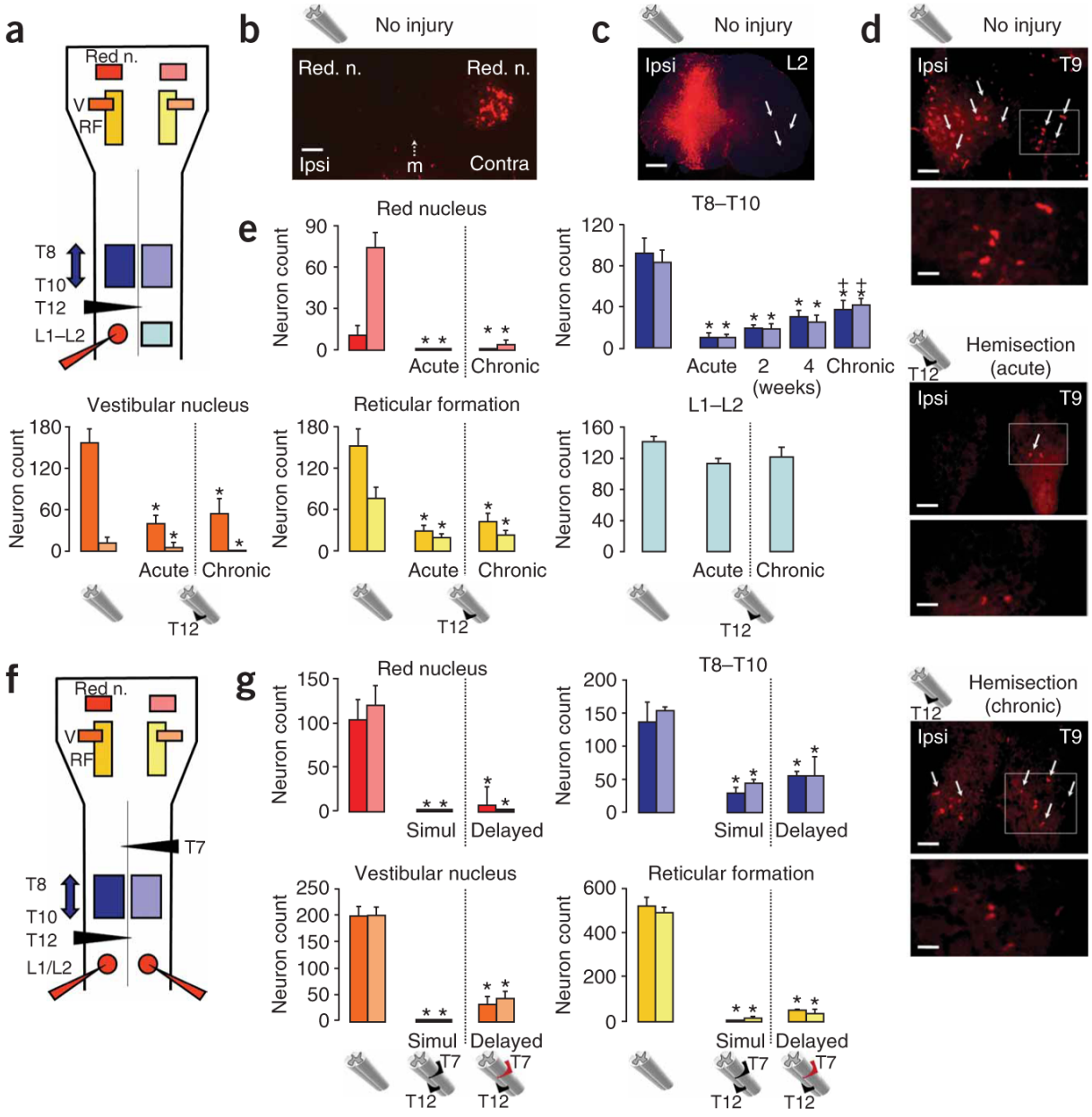

Figure 2.

Long-term loss of supraspinal but not propriospinal connections after a T12 lateral hemisection or after T12 (left) and delayed T7 (right) lateral hemisections. (**a**) Schematic of the areas evaluated in the brainstem and spinal cord after unilateral injection of retrograde tracer (Dextran–Alexa 568) at L1–L2 in uninjured mice and mice with an ipsilateral hemisection at T12. (**b–d**) Representative examples of retrograde tract tracing. (**b**) Retrogradely labeled neurons in contralateral (Contra) but not ipsilateral (Ipsi) red nucleus (n.) in an uninjured mouse. m, midline. Scale bar, 150 μm. (**c**) Tracer deposit in the unilateral injection site; arrows denote the location of retrogradely labeled neurons contralateral to the injection. Scale bar, 250 μm. (**d**) Differences in the number of retrogradely labeled neurons at T9 in uninjured mice or after the tracer was injected either immediately (acute) or at 10 weeks (chronic) after a T12 hemisection. Arrows indicate examples of tracer-labeled neurons. The areas delineated by the

boxes are shown at a higher magnification in the lower panel for each condition. Scale bars, 150 μm or 50 μm for survey or detail images, respectively. (**e**) Bar graphs showing average counts ($n = 8$ mice per group except for the acute group, $n = 6$) of retrogradely labeled neurons in the spinal cord and brainstem nuclei. (**f**) Schematic of areas evaluated in the brainstem and spinal cord after bilateral injection of retrograde tracer (Dextran–Alexa 568) at L1–L2 in mice with T12 (left) and delayed (10 weeks) T7 (right) hemisections. (**g**) Bar graphs showing the average count ($n = 6$ mice per group) of retrogradely labeled neurons in the spinal cord of and brainstem nuclei of mice injected immediately after simultaneous bilateral hemisection (Simul). Values are means ± s.e.m. $^{*}P < 0.001$, statistically significant difference compared to uninjured mice; $^{+}P < 0.01$, statistically significant difference from mice injected immediately after SCI (acute).

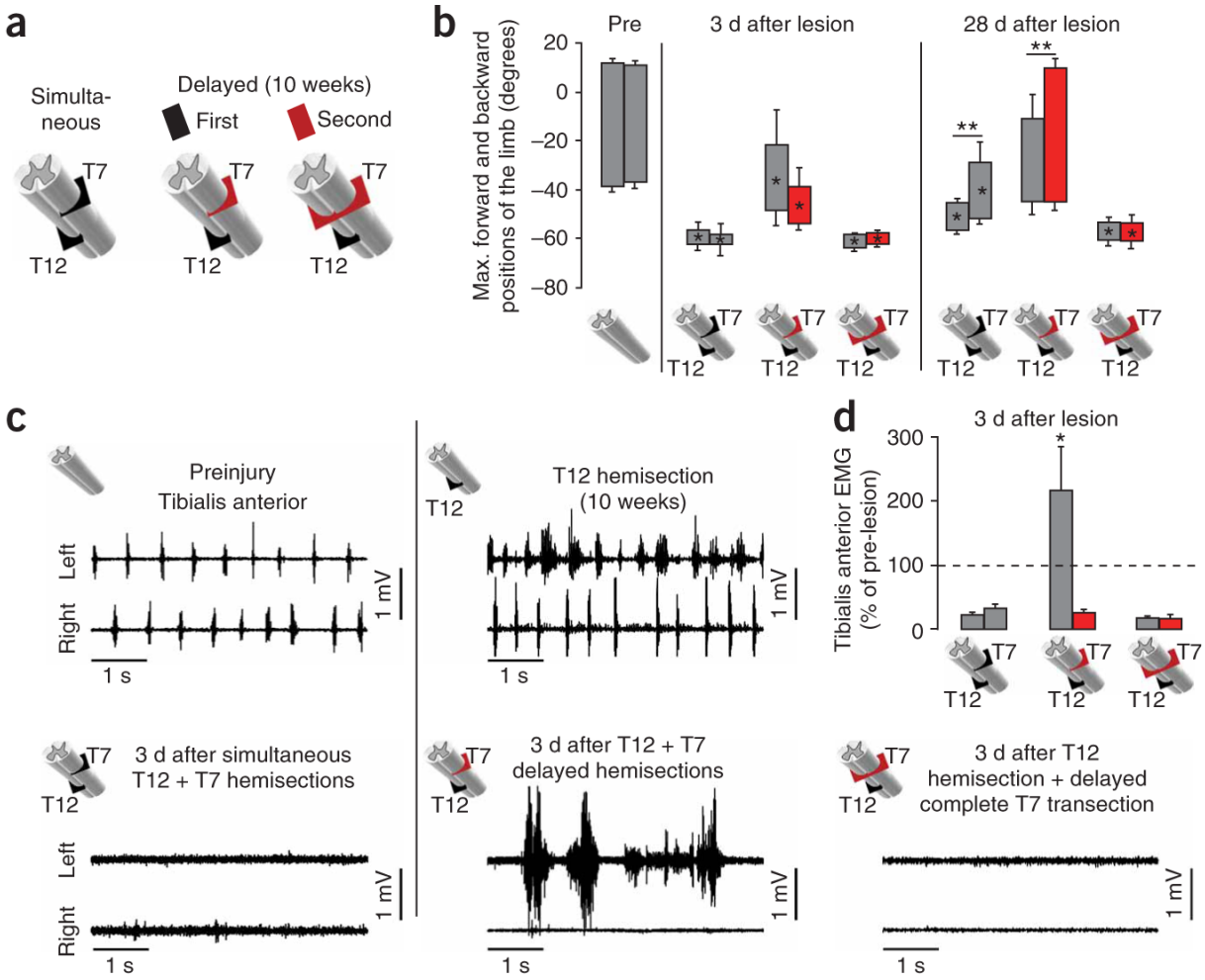

Figure 3.

Recovery of supraspinal control of stepping after delayed but not simultaneous T12 (left) and T7 (right) lateral hemisections. (**a**) Schematic of different combinations of simultaneous or delayed (10 weeks) SCIs. (**b**) Bar graphs showing the average maximum backward and forward angular positions of the limb axis after different SCIs. (**c**) Representative EMG recordings from the left and right tibialis anterior during stepping before and 3 d after different SCIs. (**d**) Bar graphs showing the average EMG burst amplitude for left and right tibialis anterior muscles ($n = 4$ for simultaneous or delayed hemisections; $n = 3$ for complete delayed T7 transection). Values are normalized to prelesion EMG activity. Values represent means ± s.e.m. $*P < 0.05$ and $**P < 0.01$, statistically significant differencs between pre- and postlesion values and between ipsilateral and contralateral hindlimbs, respectively.

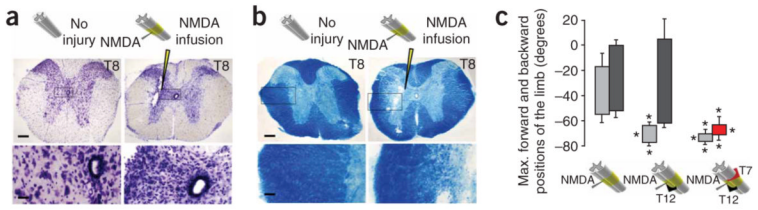

Figure 4.

Excitotoxic ablation of T8–T10 neurons abolishes the recovered control of stepping after a T12 lateral hemisection and after a T12 lateral hemisection followed by a delayed T7 lateral hemisection. (**a,b**) Survey and detail images of neighboring spinal cord sections (T8) stained for cresyl violet to show neurons (**a**) or luxol fast blue to show myelin (**b**) in uninjured mice or in mice after NMDA infusion (arrowheads). (**c**) Bar graphs showing the average maximum backward and forward angular positions of the limb axis depicted in Figure 1b during stepping 2–5 d after NMDA injection. Values represent means ± s.e.m. **P* < 0.001, statistically significant difference compared to uninjured mice. Scale bars, 170 μm and 35 μm for survey and detail images, respectively.